Functional Ecology 2002
16, 106–112

Interactions of body shape, body size and stroke-acceleration patterns in costs of underwater swimming by birds

J. R. LOVVORN*† and G. A. LIGGINS‡§

**Department of Zoology, University of Wyoming, Laramie, WY 82071, USA and ‡Department of Mechanical Engineering, University of British Columbia, Vancouver, BC V6T 1Z4, Canada*

Summary

1. For birds, mammals and turtles, costs of swimming by foot propulsion are usually much higher than for propulsion by wings or foreflippers. The propulsive efficiency with which limbs impart thrust to the water is greater for lift-based wings than for drag-based feet, but different acceleration patterns during oscillatory strokes may also alter total drag on the body fuselage (head and trunk).

2. Because wing propulsion allows thrust on both upstroke and downstroke, whereas foot propulsion in many species (perhaps excepting grebes) has little or no thrust on the upstroke, foot propulsion requires higher speeds during a smaller fraction of the stroke to maintain the same mean speed. Because drag increases non-linearly with increasing speed, higher instantaneous speeds in drag-based foot propulsion may cause greater total drag on the body fuselage.

3. Tow-tank measurements have shown that foot-propelled birds that swim with long necks extended have lower fuselage drag at high speeds than do wing-propelled birds that swim with necks retracted. This difference might reduce the higher costs of drag-based foot propulsion, but such effects must be evaluated in the context of drag at a range of speeds throughout oscillatory strokes.

4. In quasi-steady models of horizontal swimming underwater, stroke-acceleration curves for both foot and wing propulsion were applied to a range of bird shapes and sizes. Higher fuselage drag during foot propulsion increased mechanical costs of transport (MCOT, J kg^{-1} m^{-1}) by 26–40% in various species. Thus, a large fraction of the different costs of wing and foot propulsion might be explained in terms of drag on the body fuselage, independently of the propulsive efficiency of stroking limbs.

5. When drag curves for different body shapes were combined with different oscillatory stroking patterns, swimming with a long neck extended did not reduce the higher total drag associated with drag-based foot propulsion. Thus, although size and shape can affect drag measured at different constant speeds, effects of drag on locomotor costs depend much more on stroke-acceleration patterns of different swimming modes.

Key-words: Foot propulsion, oscillatory stroking, quasi-steady models, wing propulsion

Functional Ecology (2002) **16**, 106–112

Introduction

Among diving mammals, turtles and birds, two strikingly different swimming modes are evident: foot propulsion which is mostly drag-based, and wing (or foreflipper) propulsion which is mostly lift-based. At sustained speeds, costs of foot propulsion are generally much higher than for wing propulsion (Davenport, Munks & Oxford 1984; Baudinette & Gill 1985; Fish 1993, 1996; Schmid, Grémillet & Culik 1995). Wing propulsion can contain elements of drag-based thrust near the end of the power phase (Feldkamp 1987; Wyneken 1988), and foot propulsion in grebes with lobed rather than webbed toes may include lift-based thrust during the recovery phase (Johansson & Lindhe Norberg 2001). However, at sustained speeds, the propulsive efficiency with which limbs impart thrust to the water is much higher for lift-based flying (> 79%) than for drag-based paddling (< 33%) (Weihs & Webb 1983; Jackson, Locke & Brown 1992; Fish 1993).

Beyond differences in propulsive efficiency, different acceleration patterns during oscillatory strokes may

†Author to whom correspondence should be addressed. E-mail: lovvorn@uwyo.edu

§Present address: C-CORE, Memorial University of Newfoundland, St. John's, NF, Canada A1B 3X5

also alter total drag on the body fuselage (head and body trunk) (Lovvorn 2001). Wing propulsion allows thrust on both upstroke and downstroke, whereas foot propulsion in most species has little or no thrust on the upstroke. Thus, drag-based foot propulsion requires higher fuselage speeds during a smaller fraction of the stroke to maintain the same mean speed. Because drag increases non-linearly with increasing speed, higher instantaneous speeds in foot propulsion may cause greater total drag on the body fuselage.

Foot-propelled birds (loons, grebes, cormorants, ducks) often dig in sediments or search for prey in structurally complex habitats, whereas most wing-propelled birds (penguins and alcids) forage mainly in the open water column. However, some foot-propelled species commonly feed on pelagic schooling prey (Hoffman, Heinemann & Wiens 1981; Russell & Lehman 1994; Clowater 1998; Grémillet *et al*. 1998), and electronic time-depth recorders indicate dive depths and swimming speeds in cormorants as great as those of alcids or penguins of comparable size (Croxall *et al*. 1991; Williams *et al*. 1991; Schreer & Kovacs 1997). Foot-propelled birds might achieve this performance at greater locomotor cost, suggesting that they need higher foraging efficiencies than do wing-propelled species, or that other mechanisms for energy savings exist.

Regarding energy savings, tow-tank measurements show that foot-propelled birds that swim with their long necks extended (see Ross 1976) have lower fuselage drag at high speeds than do wing-propelled birds that have short necks or swim with necks retracted (Lovvorn *et al*. 2001). Because higher fuselage drag at greater instantaneous speeds might be a major reason for higher costs of foot propulsion (Lovvorn 2001), this effect of body shape on drag might lower the swimming costs of foot-propelled divers.

In this study, interactions of body shape and stroke-acceleration patterns were investigated for a range of foot-propelled and wing-propelled diving birds. In quasi-steady models, stroke-acceleration patterns were varied from having thrust distributed between upstroke and downstroke as in wing-propelled penguins and alcids, to having all thrust during the power phase as in foot-propelled ducks and cormorants. These different acceleration patterns were applied to drag curves for the frozen body fuselages of different bird species with different shapes and sizes (Lovvorn *et al*. 2001).

Materials and methods

BODY PARAMETERS AND HYDRODYNAMIC DRAG

By methods described by Lovvorn *et al*. (2001), body mass, length, surface area and maximum frontal area (calculated from maximum circumference) were measured on the same frozen specimens used in drag measurements (see below) (Table 1). Body volume V_b was calculated from curves relating body volume to body mass M_b developed for live birds of different species (Lovvorn & Jones 1991a,b). The drag of individual frozen specimens (Table 2) was measured in a tow tank by Lovvorn *et al*. (2001). Theoretically, drag is related only to the square of speed, but higher-order terms were included to fit the empirical curves exactly and thereby capture subtle effects of body shape. By analogy, according to the 'mouse-to-elephant curve', metabolic rate is related to body mass to the 0·75 power; however, individual species often show meaningful deviations from the theoretical curve developed over a very wide range of body mass. Drag curves were fitted by first ranking coefficients of multiple determination (R^2) among all possible subsets of the independent variable (speed) raised to powers up to five (α for entry into the model was 0·15; SAS Institute 1987). Plots of observed *vs* predicted values for highly ranked equations were

Table 1. Body mass M_b, added mass coefficient α, body volume V_b, body length L_b, body wetted surface area A_{sw} and maximum frontal area of individual frozen birds used in models of underwater swimming. Measurements are for wing-propelled divers (penguin, alcids) with wings removed, and for foot-propelled divers (cormorant, ducks) with legs and feet removed

Species	Species code	Added mass coeff.*	Body mass (kg)	Body volume ($m^3 \times 10^3$)	Body length (m)	Surface area (m^2)	Frontal area (m^2)
Little Penguin (*Eudyptula minor* Forster)	LIPE	0·079	0·599	0·841	0·404	0·0758	0·0052
Brünnich's Guillemot (*Uria lomvia* Linn.)	BRGU	0·075	1·268	1·917	0·444	0·0969	0·0109
Tufted Puffin (*Fratercula cirrhata* Pallas)	TUPU	0·087	0·813	1·161	0·395	0·0760	0·0077
Cassin's Auklet (*Ptychoramphus aleuticus* Pallas)	CAAU	0·075	0·182	0·282	0·210	0·0274	0·0035
Brandt's Cormorant (*Phalacrocorax penicillatus* Brandt)	BRCO	0·065	1·253	1·891	0·760	0·1287	0·0162
King Eider male (*Somateria spectabilis* Linn.)	KIEI male	0·065	1·681	2·694	0·565	0·1460	0·0162
Canvasback (*Aythya valisineria* Wilson)	CANV	0·067	0·983	1·406	0·531	0·0998	0·0100

*Based on Kochin *et al*. (1964).

Table 2. Regression equations for drag D (in N) *vs* speed U (m s^{-1}) of frozen birds. All regression coefficients were significant at $P < 0{\cdot}15$, and all coefficients of multiple determination (R^2) were $\geq 0{\cdot}999$, $P < 0{\cdot}001$. Higher-order terms represent details of shape effects on drag at different speeds

Species	Equation
Little Penguin	$D = -0{\cdot}255 + 1{\cdot}67U - 0{\cdot}387U^2 + 0{\cdot}228U^3$
Brünnich's Guillemot	$D = 1{\cdot}08 + 2{\cdot}55U^2 - 1{\cdot}38U^3 + 0{\cdot}276U^4$
Tufted Puffin	$D = 0{\cdot}230 + 3{\cdot}56U^2 - 2{\cdot}05U^3 + 0{\cdot}394U^4$
Cassin's Auklet	$D = -0{\cdot}206 + 1{\cdot}28U - 0{\cdot}267U^2 + 0{\cdot}0914U^3$
Brandt's Cormorant	$D = 1{\cdot}21 - 1{\cdot}74U + 3{\cdot}76U^2 - 1{\cdot}38U^3 + 0{\cdot}213U^4$
King Eider male	$D = 0{\cdot}457 + 1{\cdot}33U + 0{\cdot}944U^2$
Canvasback	$D = 0{\cdot}703 - 0{\cdot}854\mathrm{U} + 2{\cdot}65\mathrm{U}^2 - 0{\cdot}801\mathrm{U}^3 + 0{\cdot}0899\mathrm{U}^4$

Table 3. Mean speeds and stroke periods (1/stroke frequency) used in simulations of steady horizontal swimming underwater (without glide phases between strokes). See text for data sources

Species	Mean speed (m s^{-1})	Stroke period (s)
Little Penguin	1·66	0·284
Brünnich's Guillemot	1·6	0·357
Tufted Puffin	1·45	0·324
Cassin's Auklet	1·2	0·268
Brandt's Cormorant	1·5	0·345
King Eider male	1·4	0·340
Canvasback	0·93	0·278

then visually inspected to select the equation showing the fewest deviations. All simulations in this paper were for horizontal swimming, so work against buoyancy was not considered (cf. Lovvorn, Croll & Liggins 1999; Lovvorn 2001).

MEAN SPEEDS AND STROKE PERIODS

Mean underwater swimming speeds U and stroke periods P_s (1/stroke frequency) were drawn from studies of captive birds in dive tanks, or of free-ranging birds with time-depth recorders (TDRs) or speed gauges, and extrapolated to unstudied species (Table 3). Clark & Bemis (1979) reported means (± SD) of $U = 1{\cdot}66 \pm 0{\cdot}10$ m s^{-1} and $P_s = 0{\cdot}284 \pm 0{\cdot}019$ s for Little Penguins ($n = 7$) swimming horizontally in tanks. Based on speed gauges, Gales, Williams & Ritz (1990) reported means for free-ranging Little Penguins of 2·3–2·4 m s^{-1}, but these values included periods of pursuing prey and perhaps porpoising at higher speeds (cf. Wilson & Wilson 1990; Luna Jorquera 1996). Mean speeds during direct descent and ascent of Brünnich's Guillemots based on TDRs, regardless of depth and buoyancy, are 1·5–1·6 m s^{-1} (Lovvorn *et al*. 1999); we used 1·6 m s^{-1} for horizontal speed. Stroke duration of guillemots is about 0·357 s (Lovvorn *et al*. 1999). Swimming speeds of puffins and auklets have not been studied; we assumed 1·45 m s^{-1} for Tufted Puffins relative to body mass and observations for Rhinoceros Auklets (*Cerorhinca monocerata* Pallas; Burger *et al*. 1993), and 1·2 m s^{-1} for Cassin's Auklets (Burger & Powell 1990). Stroke periods were linearly scaled to that of guillemots according to relative speeds to yield 0·324 s for Tufted Puffins and 0·268 s for Cassin's Auklets. Mean vertical speeds during descent and ascent have been measured with TDRs for various cormorant species (Croxall *et al*. 1991; Kato *et al*. 1996; Watanuki, Kato & Naito 1996; Wanless *et al*. 1997). These studies indicate typical swimming speeds of about 1·5 m s^{-1} (J. R. Lovvorn, A. Kato, Y. Watanuki & Y. Naito, unpublished data), which agrees with the mean horizontal speed of 1·51 m s^{-1} of Great Cormorants (*Phalacrocorax carbo* Linn.) in a diving tank (Schmid *et al*. 1995); 1·5 m s^{-1} was used for Brandt's Cormorants. Lacking data on stroke periods of cormorants, $P_s = 0{\cdot}345$ s was assumed. For Canvasbacks, we used means of $U = 0{\cdot}93$ m s^{-1} and $P_s = 0{\cdot}278$ s measured during descent in tanks, and used body-size scaling for other diving duck species (Lovvorn 1994) to estimate values of 1·4 m s^{-1} and 0·340 s for male King Eiders (Table 3). (There is substantial size difference between sexes in King Eiders.) Note that speeds of actively feeding birds can be higher than mean speeds during non-feeding periods of travel used here (Swennen & Duiven 1991; Burger *et al*. 1993; Luna Jorquera 1996).

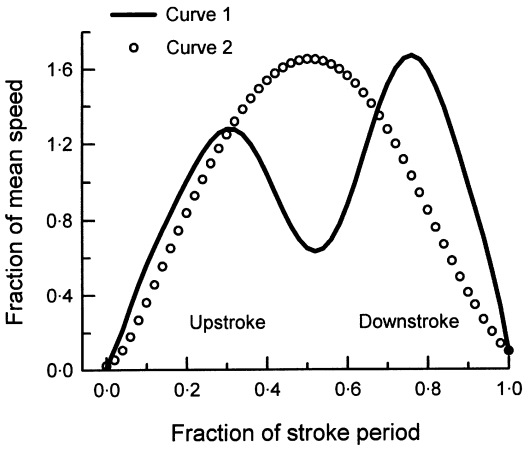

Fig. 1. Relations between fraction of mean swimming speed F_U and fraction of stroke period F_P used in simulations of underwater swimming by birds. Curve 1 for wing propulsion is based on thrust calculations for Humboldt Penguins swimming horizontally underwater at 1 m s^{-1} (Hui 1988; Lovvorn *et al*. 1999). Upstroke and downstroke parts of the curve for wing propulsion are labeled. Curve 2 for foot-propelled divers is from Canvasbacks during descent (Lovvorn *et al*. 1991). For equations of curves, see text.

STROKE ACCELERATION CURVES, INERTIAL WORK AND SUMMATION OF WORK COMPONENTS

Representative curves of changes in speed throughout swimming strokes (Fig. 1) were used to calculate time-varying acceleration to be applied to different body shapes. Curve 1 (Fig. 1) was based on calculated thrust throughout a stroke for Humboldt Penguins (*Spheniscus humboldti* Meyen; Hui 1988; see details in Lovvorn *et al*. 1999). Curve 2 was based on high-speed

films of foot-propelled Canvasbacks descending in a tank (Lovvorn, Jones & Blake 1991). Equations for these curves relating fraction of mean speed F_U to fraction of stroke period F_P (Fig. 1) were $F_U = 0{\cdot}07403 - 1{\cdot}0396F_P + 184{\cdot}12F_P^2 - 2250{\cdot}68F_P^3 + 14\,114F_P^4 - 49\,819F_P^5 + 100\,308F_P^6 - 11\,1428F_P^7 + 57\,188F_P^8 - 9600{\cdot}88F_P^{10} + 1304{\cdot}89F_P^{12}$ for Curve 1, and $F_U = 0{\cdot}03595 - 0{\cdot}35734F_P + 67{\cdot}9108F_P^2 - 472{\cdot}11F_P^3 + 1979{\cdot}33F_P^4 - 5327{\cdot}65F_P^5 + 8996{\cdot}62F_P^6 - 9033{\cdot}24F_P^7 + 4435{\cdot}99F_P^8 - 761{\cdot}29F_P^{10} + 114{\cdot}86F_P^{12}$ for Curve 2. As for drag curves (see above), these high-order equations were used to achieve exact fits to the empirical curves, based on stepwise multiple regression (all coefficients were significant at $\alpha = 0{\cdot}1$) and visual inspection of results.

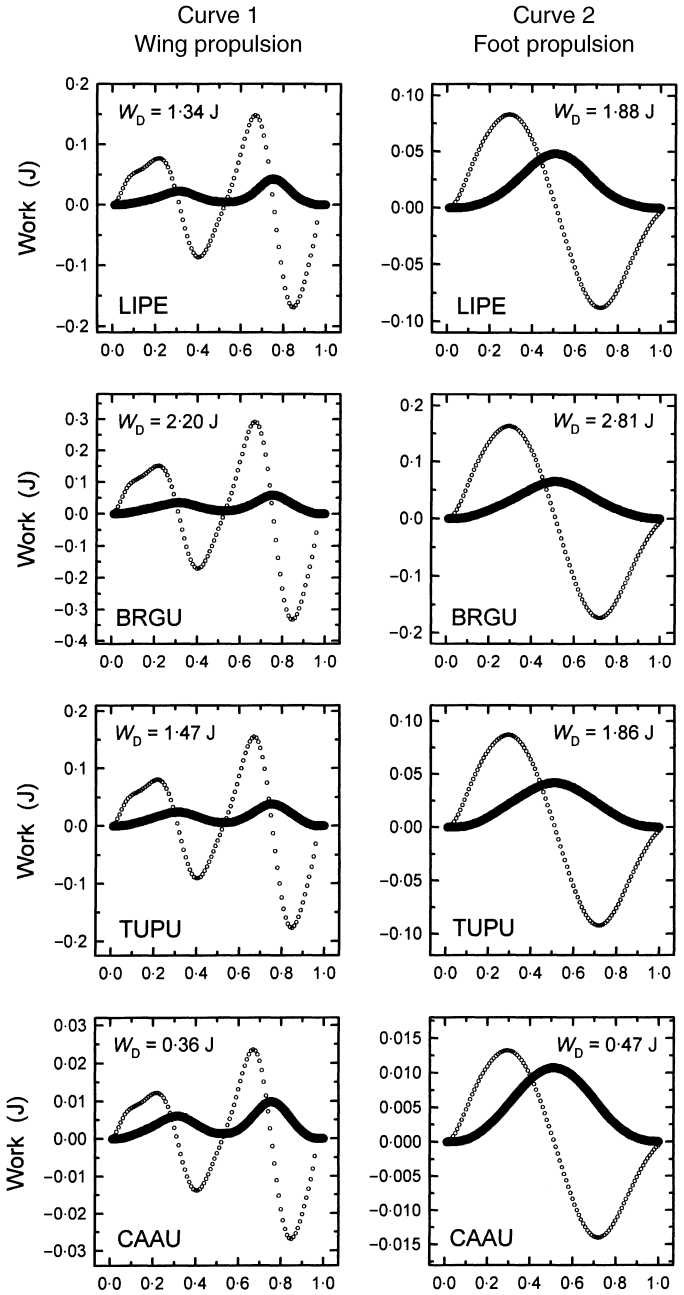

Fig. 2. Mechanical work against drag (solid line) and to accelerate the body fuselage (open circles) throughout a single stroke during steady horizontal swimming underwater (without glide phases between strokes) by wing-propelled birds. Patterns are shown for two acceleration curves (Fig. 1) for each bird species. Total drag work W_D is shown for each stroke. Species codes are in Table 1.

Added mass M_a is the mass of entrained water accelerated along with the mass of the body M_b during swimming strokes (Daniel 1984; Denny 1988). The added mass coefficient α (ratio of added volume of water to body volume, Table 1) was estimated from plots relating α to ratios of the three axes of ellipsoids moving in the direction of the longest axis (Fig. 150 in Kochin, Kibel & Roze 1964). The effective body length (total length minus length of culmen) was used for the long axis (Aleyev 1977), and the maximum height and width of the body for the other axes. Added mass was calculated as $M_a = \alpha\rho V_b$, where ρ is the density of fresh water at 20 °C (998·1 kg m^{-3}). The force g required to accelerate the virtual mass (body mass plus added mass) was calculated as $g = -(M_b + M_a)(dU/dt)$, where dU/dt is the change in speed over intervals of 0·01 s (see below). Added mass coefficients (Table 1) increased as the frontal cross-section became less circular and more elliptical (gradient from penguin to cormorant, see Fig. 1 in Lovvorn *et al.* 2001), thereby increasing the relative maximum diameter.

Work throughout swimming strokes was modelled by calculating the linear distance moved by the body fuselage during 0·01-s intervals, according to fractional (Fig. 1) and mean (Table 3) speeds and periods. Inertial (accelerational) work was the work done to accelerate the body and the added mass of entrained water over each 0·01-s interval. Drag work was calculated by multiplying drag by displacement during the same interval. A quasi-steady modelling approach was used, in which drag of the fuselage for a given interval during the stroke is assumed to be the same as drag at that speed under steady conditions. In quasi-steady fashion, both inertial and drag work during all 0·01-s intervals was then integrated over the entire stroke to yield total work during the stroke (Lovvorn *et al.* 1991, 1999).

Results

The two stroke-acceleration curves (Fig. 1) were applied to each species to investigate interactions between body shape and stroke-acceleration pattern. Because positive work of acceleration and negative work of deceleration mostly cancel during horizontal swimming at constant speed, and work against buoyancy during horizontal swimming was not considered, essentially all net work was against drag. For penguins and alcids that have short necks or swim with necks retracted, patterns of work against drag and to accelerate the body fuselage during a stroke were similar among species for different acceleration curves (Fig. 2), except that drag was relatively greater in the smaller species (Little Penguin and Cassin's Auklet). Work against drag on the body fuselage increased dramatically when thrust occurred only during the power phase as in drag-based foot propulsion (Curve 2).

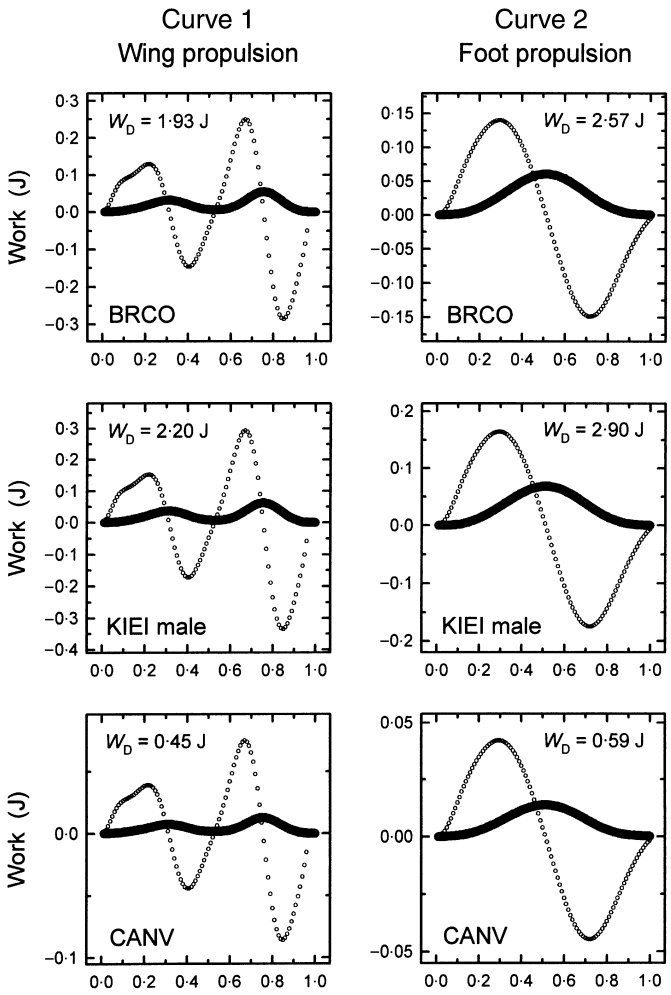

Fig. 3. Mechanical work against drag (solid line) and to accelerate the body fuselage (open circles) throughout a single stroke during steady horizontal swimming underwater (without glide phases between strokes) by foot-propelled birds. Patterns are shown for two acceleration curves (Fig. 1) for each bird species. Total drag work W_D is shown for each stroke. Species codes are in Table 1.

Patterns of work for different acceleration curves were very similar among foot-propelled species that swim with long necks extended (Fig. 3). Curves for foot-propelled and wing-propelled species of similar body mass showed close resemblance (cf. Brünnich's Guillemot in Fig. 2 *vs* Brandt's Cormorant and male King Eider in Fig. 3). As for wing-propelled species, the fuselage drag of foot-propelled species was substantially higher when Curve 2 for foot propulsion was applied to them. The increase in drag work and associated mechanical cost of transport (MCOT, J kg^{-1} m^{-1}) varied from 26 to 40% in different species (Fig. 4). However, there was no consistent evidence that the long thin shape of the foot-propelled divers reduced the higher drag work and MCOT associated with foot propulsion, or that trends in the increase varied with body size (Fig. 4).

Discussion

For horizontal swimming underwater at constant mean speed, and without glide phases between strokes (Lovvorn 2001), total drag work and MCOT were 26–40% higher when stroke-acceleration curves for drag-based foot propulsion *vs* wing propulsion were applied to the same bird species (Fig. 4). These increases resulted solely from greater drag on the body fuselage during the higher instantaneous speeds of drag-based foot propulsion, and are independent of the higher propulsive efficiency by which lift-based wings impart thrust to the water (see Weihs & Webb 1983; Fish 1993, 1996). Despite variation among species, there were no consistent effects of body size, or of swimming with long extended necks *vs* short or retracted necks (Fig. 4c).

Our simulations considered only mechanical and not aerobic costs. In the only empirical comparison for birds to date, the oxygen consumption of Great Cormorants swimming horizontally underwater in tanks was 2·7 times that of Adélie Penguins (*Pygoscelis adeliae* Hombron and Jacquinot) (Schmid *et al*. 1995). With aerobic efficiency (mechanical power output/aerobic power input) of 25% or less, a large fraction of this difference in cost could result from 26 to 40% greater work against drag on the body fuselage due to higher instantaneous speeds of drag-based foot propulsion (Fig. 4c).

Bannasch (1993) found that the drag of cast models of Pygoscelid Penguins closely resembled that of an axisymmetric body of revolution of similar dimensions, in which fully turbulent flow was induced by a wire around the front of the model. In comparing penguins with known streamlined shapes, Nachtigall & Bilo (1980) concluded that the drag coefficients of penguins based on frontal area and volume could not be improved. Nevertheless, computer simulations suggested that more elongated shapes might have even lower drag (Pinebrook 1982). Tow-tank measurements indicated that species that swim with long necks extended (cormorants and ducks) have lower drag at high speeds (and higher drag at low speeds) than do birds with short necks or that swim with necks retracted (penguins and alcids; Lovvorn *et al*. 2001). However, birds do not actually swim at constant speed, but rather at a wide range of instantaneous speeds during accelerational strokes (Fig. 1). In the latter context, our quasi-steady model indicated that body-shape effects on drag at different speeds had no consistent effect on the cost of entire strokes.

Foot propulsion in grebes might include significant elements of lift-based thrust (Johansson & Lindhe Norberg 2001). Grebes differ from loons, ducks and cormorants in having lobed (rather than webbed) toes that may cant independently to maximize lift (Johansson & Lindhe Norberg 2000). As yet, there have been no calculations for grebes of the amount or fraction of thrust generated by lift- *vs* drag-based mechanisms throughout a stroke cycle (cf. Jackson *et al*. 1992), and the canted-toe mechanism is not possible in web-toed species. Analyses in this paper are not intended to estimate the work done by different species (such as grebes) according to their unique stroke-acceleration patterns. Rather, we have evaluated the potential importance of size and shape effects on drag measured at steady speeds to the costs

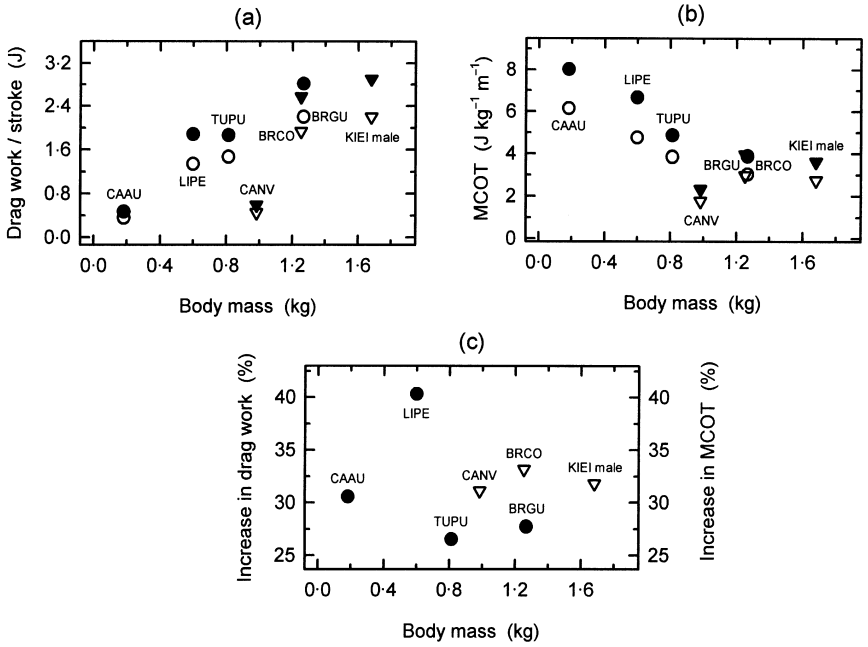

Fig. 4. (a) Comparison of drag work per stroke for steady horizontal swimming underwater (without glide phases between strokes), when acceleration Curve 1 (for wing propulsion, open symbols) and Curve 2 (for foot propulsion, closed symbols) (Fig. 1) are both applied to wing-propelled (circles) and foot-propelled (triangles) species. (b) Mechanical costs of transport (MCOT, J kg^{-1} m^{-1}) corresponding to drag values in part (a). (c) Percentage increase in drag work and MCOT for each species when acceleration Curve 2 is used rather than Curve 1 for wing-propelled (circles) and foot-propelled (triangles) species, based on data in parts (a) and (b). Species codes are in Table 1.

of oscillatory, accelerational swimming. By applying stroke-acceleration curves for the extremes of drag-based *vs* lift-based propulsion, we have shown that although fuselage drag at steady speeds varies with shape among species (Lovvorn *et al*. 2001), such effects are minimal compared to effects on total drag of the higher instantaneous speeds during drag-based foot propulsion. Our conclusion is that this extra cost of foot propulsion is not appreciably mitigated by different sizes or shapes of the body fuselage.

Despite higher mechanical cost of transport (MCOT) during steady swimming (Fig. 4b), foot propulsion may allow greater manoeuvrability (lunging, braking, turning) at lower speeds, and may be more suitable for hovering over and probing benthic substrates (Lindroth & Bergstöm 1959; Duffy, Todd & Siegfried 1987; Wyneken 1988). However, manoeuvrability is probably not greater for foot than wing propulsion at high speeds (Allen 1926; Spring 1971; Hui 1985), and the cost of direct dives to appreciable depths is probably higher for more unsteady drag-based foot propulsion than by wing propulsion (cf. Lovvorn 2001). Marine cormorants, which have partially wettable plumage and may have exceptional heat loss in cold water, have geographical ranges that extend into polar environments dominated by alcids or penguins. Cormorants apparently meet this thermoregulatory challenge by finding situations (prey size, density, depth, visibility) where food intake rates are high enough to offset costs (Grémillet *et al*. 1999a,b), or by having better prey-capture methods. For feeding on pelagic schooling prey or at deep depths, our analyses suggest that similar compensatory strategies are needed by cormorants and other foot-propelled divers to offset the higher costs of drag-based foot propulsion.

Acknowledgements

We thank G. V. Byrd, P. Dann, M. B. Decker, D. A. Dorado, G. L. Hunt and J. Williams for obtaining bird specimens, S. M. Calisal for laboratory space and helpful suggestions, and D. R. Jones for humour and inspiration. This research was supported by US National Science Foundation grant OPP-9813979 to JRL.

References

Aleyev, Y.G. (1977) *Nekton*. Dr W. Junk Publishers, The Hague.

Allen, W.E. (1926) The diving of the Rhinoceros Auklet. *Bird-Lore* **28**, 331–332.

Bannasch, R. (1993) Drag minimisation on bodies of revolution in nature and engineering. *Proceedings of the International Airship Conference*, pp. 79–87. Universität Stuttgart, Stuttgart, Germany.

Baudinette, R.V. & Gill, P. (1985) The energetics of 'flying' and 'paddling' in water: locomotion in penguins and ducks. *Journal of Comparative Physiology B* **155**, 373–380.

Burger, A.E. & Powell, D.W. (1990) Diving depths and diet of Cassin's Auklet at Reef Island, British Columbia. *Canadian Journal of Zoology* **68**, 1572–1577.

Burger, A.E., Wilson, R.P., Garnier, D. & Wilson, M.-P.T. (1993) Diving depths, diet, and underwater foraging of Rhinoceros Auklets in British Columbia. *Canadian Journal of Zoology* **71**, 2528–2540.

Clark, B.D. & Bemis, W. (1979) Kinematics of swimming of penguins at the Detroit Zoo. *Journal of Zoology, London* **188**, 411–428.

Clowater, J.S. (1998) *Distribution and foraging behaviour of wintering Western Grebes*. MS Thesis, Simon Fraser University, Burnaby, BC, Canada.

Croxall, J.P., Naito, Y., Kato, A., Rothery, P. & Briggs, D.R. (1991) Diving patterns and performance in the Antarctic Blue-eyed Shag *Phalacrocorax atriceps*. *Journal of Zoology, London* **225**, 177–199.

Daniel, T.L. (1984) Unsteady aspects of aquatic locomotion. *American Zoologist* **24**, 121–134.

Davenport, J., Munks, S.A. & Oxford, P.J. (1984) A comparison of the swimming of marine and freshwater turtles. *Proceedings of the Royal Society of London B* **220**, 447–475.

Denny, M.W. (1988) *Biology and the Mechanics of the Wave-Swept Environment*. Princeton University Press, Princeton, NJ.

Duffy, D.C., Todd, F.S. & Siegfried, W.R. (1987) Submarine foraging behavior of alcids in an artificial environment. *Zoo Biology* **6**, 373–378.

Feldkamp, S.D. (1987) Foreflipper propulsion in the California sea lion, *Zalophus californianus*. *Journal of Zoology, London* **212**, 43–57.

Fish, F.E. (1993) Influence of hydrodynamic design and propulsive mode on mammalian swimming energetics. *Australian Journal of Zoology* **42**, 79–101.

Fish, F.E. (1996) Transitions from drag-based to lift-based propulsion in mammalian swimming. *American Zoologist* **36**, 628–641.

Gales, R., Williams, C. & Ritz, D. (1990) Foraging behaviour of the Little Penguin, *Eudyptula minor*: initial results and assessment of instrument effect. *Journal of Zoology, London* **220**, 61–85.

Grémillet, D., Argentin, G., Schulte, B. & Culik, B.M. (1998) Flexible foraging techniques in breeding Cormorants *Phalacrocorax carbo* and Shags *Phalacrocorax aristotelis*: benthic or pelagic feeding? *Ibis* **140**, 113–119.

Grémillet, D., Wilson, R.P., Storch, S. & Yann, G. (1999a) Three-dimensional space utilization by a marine predator. *Marine Ecology Progress Series* **183**, 263–273.

Grémillet, D., Wilson, R.P., Wanless, S. & Peters, G. (1999b) A tropical bird in the Arctic (the cormorant paradox). *Marine Ecology Progress Series* **188**, 305–309.

Hoffman, W., Heinemann. D. & Wiens, J.A. (1981) The ecology of seabird feeding flocks in Alaska. *Auk* **98**, 437–456.

Hui, C.A. (1985) Maneuverability of the Humboldt Penguin (*Spheniscus humboldti*) during swimming. *Canadian Journal of Zoology* **63**, 2165–2167.

Hui, C.A. (1988) Penguin swimming. I. Hydrodynamics. *Physiological Zoology* **61**, 333–343.

Jackson, P.S., Locke, N. & Brown, P. (1992) The hydrodynamics of paddle propulsion. *Australasian Fluid Mechanics Conference* **11**, 1197–1200.

Johansson, L.C. & Lindhe Norberg, U.M. (2000) Asymmetric toes aid underwater swimming. *Nature* **407**, 582–583.

Johansson, L.C. & Lindhe Norberg, U.M. (2001) Lift-based paddling in diving grebe. *Journal of Experimental Biology* **204**, 1687–1696.

Kato, A., Naito, Y., Watanuki, Y. & Shaughnessy, P.D. (1996) Diving pattern and stomach temperatures of foraging King Cormorants at subantarctic Macquarie Island. *Condor* **98**, 844–848.

Kochin, N.E., Kibel, I.A. & Roze, N.V. (1964) *Theoretical Hydromechanics*. Wiley, New York.

Lindroth, A. & Bergstöm, E. (1959) Notes on the feeding technique of the Goosander in streams. *Report of the Institute of Freshwater Research, Drottningholm* **40**, 165–175.

Lovvorn, J.R. (1994) Biomechanics and foraging profitability: an approach to assessing trophic needs and impacts of diving ducks. *Hydrobiologia* **279/280**, 223–233.

Lovvorn, J.R. (2001) Upstroke thrust, drag effects, and stroke-glide cycles in wing-propelled swimming by birds. *American Zoologist* **41**, 154–165.

Lovvorn, J.R. & Jones, D.R. (1991a) Effects of body size, body fat, and change in pressure with depth on buoyancy and costs of diving in ducks (*Aythya* spp.). *Canadian Journal of Zoology* **69**, 2879–2887.

Lovvorn, J.R. & Jones, D.R. (1991b) Body mass, volume, and buoyancy of some aquatic birds, and their relation to locomotor strategies. *Canadian Journal of Zoology* **69**, 2888–2892.

Lovvorn, J.R., Jones, D.R. & Blake, R.W. (1991) Mechanics of underwater locomotion in diving ducks: drag, buoyancy and acceleration in a size gradient of species. *Journal of Experimental Biology* **159**, 89–108.

Lovvorn, J.R., Croll, D.A. & Liggins, G.A. (1999) Mechanical *versus* physiological determinants of swimming speeds in diving Brünnich's Guillemots. *Journal of Experimental Biology* **202**, 1741–1752.

Lovvorn, J.R., Liggins, G.A., Borstad, M.H., Calisal, S.M. & Mikkelsen, J. (2001) Hydrodynamic drag of diving birds: effects of body size, body shape and feathers at steady speeds. *Journal of Experimental Biology* **204**, 1547–1557.

Luna Jorquera, G. (1996) *Balancing the energy budget for a warm-blooded bird in a hot desert and cold seas: the case of the Humboldt Penguin.* PhD Thesis, University of Kiel, Kiel, Germany.

Nachtigall, W. & Bilo, D. (1980) Strömungsanpassung des pinguins beim schwimmen unter wasser. *Journal of Comparative Physiology A* **137**, 17–26.

Pinebrook, W.E. (1982) *Drag minimization on a body of revolution*. PhD Thesis, University of Houston, Houston, TX.

Ross, R.K. (1976) Notes on the behavior of captive Great Cormorants. *Wilson Bulletin* **88**, 143–145.

Russell, R.W. & Lehman, P.E. (1994) Spring migration of Pacific Loons through the Southern California Bight: nearshore flights, seasonal timing and distribution at sea. *Condor* **96**, 300–315.

SAS Institute (1987) *SAS/STAT Guide for Personal Computers*, Version 6 edition. SAS Institute, Cary, NC.

Schmid, D., Grémillet, D.J.H. & Culik, B.M. (1995) Energetics of underwater swimming in the Great Cormorant (*Phalacrocorax carbo sinensis*). *Marine Biology* **123**, 875–881.

Schreer, J.F. & Kovacs, K.M. (1997) Allometry of diving capacity in air-breathing vertebrates. *Canadian Journal of Zoology* **75**, 339–358.

Spring, L. (1971) A comparison of functional and morphological adaptations in the common murre (*Uria aalge*) and Thick-billed Murre (*Uria lomvia*). *Condor* **73**, 1–17.

Swennen, C. & Duiven, P. (1991) Diving speed and food-size selection in Common Guillemots, *Uria aalge*. *Netherlands Journal of Sea Research* **27**, 191–196.

Wanless, S., Harris, M.P., Burger, A.E. & Buckland, S.T. (1997) Use of time-at-depth recorders for estimating depth and diving performance of European Shags. *Journal of Field Ornithology* **68**, 547–561.

Watanuki, Y., Kato, A. & Naito, Y. (1996) Diving performance of male and female Japanese Cormorants. *Canadian Journal of Zoology* **74**, 1098–1109.

Weihs, D. & Webb, P.W. (1983) Optimization of locomotion. *Fish Biomechanics* (eds P. W. Webb & D. Weihs), pp. 339–371. Praeger, New York.

Williams, T.D., Croxall, J.P., Naito, Y. & Kato, A. (1991) Diving patterns and processes in epipelagic and benthic foraging sub-antarctic seabirds. *Proceedings of the International Ornithological Congress* **20**, 1393–1401.

Wilson, R.P. & Wilson, M.-P.T. (1990) Foraging ecology of breeding *Spheniscus* penguins. *Penguin Biology* (eds L. S. Davis & J. T. Darby), pp. 181–206. Academic Press, San Diego, CA.

Wyneken, J. (1988) *Comparative and functional considerations of locomotion in turtles*. PhD Thesis, University of Illinois, Urbana-Champaign, USA.

Received 17 January 2001; revised 15 August 2001; accepted 22 August 2001